Publisher homepage: www.universepg.com, ISSN: 2707-4625 (Online) & 2707-4617 (Print)

https://doi.org/10.34104/ijmms.024.01120119

International Journal of Material and Mathematical Sciences

Journal homepage: www.universepg.com/journal/ijmms

Heat Transfer Analysis Using Synthesized Silver Nanoparticles

Mohammad Arif Shahriar[1], Md. Aminul Islam[1]*, and Shantanu Saha[1]

[1]Department of Mechanical Engineering, Chittagong University of Engineering & Technology, Chittagong - 4349, Bangladesh.

*Correspondence: aislam@cuet.ac.bd (Md. Aminul Islam, Department of Mechanical Engineering, Chittagong University of Engineering & Technology, Chittagong - 4349, Bangladesh).

Received Date: 19 July 2024 Accepted Date: 20 August 2024 Published Date: 27 August 2024

ABSTRACT

Silver nanoparticles were synthesized via the sol-gel method from different concentrations of silver nitrate and the reducing agent hydrazine hydrate in the presence of citric acid and silver nitrate. The synthesized silver nanoparticles are then separated by evaporation through the addition of heat at 100°C. Three samples of nanoparticles were prepared and tested through XRD to ensure that the particle size reached the nanoscale (1 nm-100 nm). The sizes of the synthesized nanoparticles in the 1st, 2nd, and 3rd samples were 15 nm, 20 nm and 21 nm, respectively, and the average size was 19 nm. Nanofluids are prepared by mixing nanoparticles through ultrasonication with a base fluid (water), and the heat transfer coefficient of the nanofluids is measured in a shell and tube heat exchanger. The heat transfer coefficient of the base fluid (water) was 2926.85 W/(m^{2}K), and the heat transfer coefficients with nanoparticles were 4928.22 W/(m^{2}K), 5125.26 W/(m^{2}K), and 4629.254 W/(m^{2}K). The increases in the heat transfer coefficient for the 1st, 2nd, and 3rd samples are 68%, 75%, and 58%, respectively, greater than that of the base fluid.

Keywords: Ag Nanoparticles, Heat transfer, Silver nanoparticles, and Nanofluid.

INTRODUCTION:

Due to the limitations of macro- and microparticles, researchers had to prepare suspensions of nanoparticles and found that copper nanofluids were three times more conductive than water was (S. K. Das *et al.,* 2006). The reason behind these characteristics arises because the surface area of the same usual volume greatly increases; for example, 1 kg of 1 mm^3 particles has the same surface area as 1 mg of 1 nm^3 particles (King *et al.,* 2024). Nanofluids aim to maximize thermal properties while using minimal concentrations (ideally less than 1% by volume). This is achieved by uniformly dispersing and stably suspending nanoparticles (preferably smaller than 10 nanometers) within the host fluids (Choi, 2008).

Different sol-gel synthesis methods include bioactive metal nanoparticles (BGNs), base-catalyzed methods (the Stöber method), acid/base catalyzed methods, post modification of sol-gel derived nanoparticles, microemulsion-assisted sol-gel methods, aerosol-assisted sol-gel methods and many other sol-gel-based methods (Zheng & Boccaccini, 2017). The synthesis of bioactive metal nanoparticles (BGNs) has numerous advantages, and options, for example, Ag-silica nanocomposites, were synthesized by applying acetonitrile bifunctionally as a solvent and metal ion stabilizer with high concentrations of Ag nanoparticles without the use of silicon alkoxide to settle metal ions. This process has also been used for "block copolymer-directed self-assembly of mesoporous material, spin coating of film and electrospinning of nanofibers". In addition, many organic and inorganic hybrid nanoparticles can be synthesized by UV radiation or hydrolytic sol-gel

methods (Chibac *et al.,* 2012). Silver nanoparticles are synthesized through a number of processes and methods that are repeatedly used by researchers for different purposes. Physical methods could include elector deposition or an explosion wire process. The nanoparticles were 16 nm in size, which is smaller than most other methods described in other papers (Solanki & Murthy, 2011). Chemical methods are among the most used methods for synthesizing nanoparticles. Silver nanoparticles synthesized in two solvents with special microscopic irradiation wavelengths of 7 and 12 nm had the same efficiency as synthesized nanoparticles synthesized via other methods, and the synthesized Ag colloids were stable for 6 months. It was possible to produce a monolayer of AgNPs of 48 nm with modified substrates of macrocations (Michna *et al.,* 2019; Noroozi *et al.,* 2014; Islam *et al.,* 2020). Green synthesis has recently become the most effective method for producing nanoparticles because of its natural availability and environmental friendliness. Crystal-ized nanoparticles of various sizes can be produced from the biomass of Spirulina platensis, the leaf extract of Enicostemma axillare (Lam.), inside the human gut, the algae Botryo-coccus braunii, Poulownia tomentosa tree, silkworm cocoon fibroins and Penicillium cyclopium were found (Arya *et al.,* 2019; Bian *et al.,* 2019; Cui *et al.,* 2018; Escobar-Hernández & Escobar-Remolina, 2019; Mahdieh *et al.,* 2012; Pontaza-Licona *et al.,* 2019; Raj *et al.,* 2018; Wanarska & Maliszewska, 2019).

Graphene nanofluids increase the heat transfer rate by 29% at 450°C with different power inputs, temperatures and angles of inclination (S. Das *et al.,* 2019). Compared with those of the base fluid, heat transfer via silver nanoparticles of 0.1% and 0.3% at 40°C enhanced heat transfer by approximately 18% and 5%, respectively (Rodrigues *et al.,* 2014). In an experiment with two sizes of silver nanoparticles and oil as the mixing fluid, the heat transfer increment was approximately 30% in laminar flow and increased further with increasing Reynolds number (Hosseini & Ghorbani, 2018). The heat transfer enhancement of hybrid nanofluids works in both laminar and turbulent flows (Huminic & Huminic, 2018). Several researchers have synthesized 9 kinds of nanoparticles by chemical solution methods with controllable microstructures, and the addition of a low thermal conductivity liquid can also strongly increase heat transfer (Wang & Wei, 2009). Silicon dioxide–water nanofluids with a diameter of 20 nm were used to measure the heat transfer coefficient and pressure drop compared to those of water alone. They concluded that using nanofluids results in a pressure drop higher than that of only the base fluid, which may limit the use of these nanofluids (Anoop *et al.,* 2013). Several studies of magnetic impact and different temperatures utilizing water as the base fluid and 0.112 vol.% Cu/CuO nanoparticles have shown that the same experiment can be reproduced using the maximum magnetic field influence (Roszko *et al.,* n.d.).

METHOLODOGY:

Most silver nanoparticle synthesis processes are green because of their antibacterial properties. The majority of metal chemical processes in nanoparticle synthesis begin with the reduction of metal alkoxides, which is a common beginning step for sol-gel method. In this process, the initial molecular precursor (typically a metal alkoxide) dissolves in water or alcohol. Then, through heating and stirring, it transforms into a gel via hydrolysis or alcoholysis (Bokov *et al.,* 2021). Silver alkoxides are not as abundant as other metal alkoxides; rather, they can be classified as rare (Edworthy *et al.,* 2005).

Therefore, different other methods are utilized to synthesize silver nanoparticles in the sol-gel process. Several chemical reduction methods are also available, from which a synthesis technique per-formed at room temperature was chosen. The reducer concentration and silver nitrate concentration were varied to determine the effect of these concentrations on the particle size. Later, these nanoparticles were mixed with water as the base fluid to produce nanofluids. The heat transfer coefficient of the nanofluid sample was measured using a shell and tube heat exchanger.

Silver nanoparticle synthesis

The nanoparticles were prepared by mixing silver nitrate ($AgNO_3$), citric acid ($C_6H_8O_7$), sodium hydro-xide (NaOH), and ammonia (NH_3), which was used to adjust the pH to neutral, as per the flow diagram shown in **Fig. 1**.

Silver ion reduction was confirmed when the solution turned black and the solution was evaporated in the presence of hydrazine hydrate, which acted as a reducing agent to separate the nanoparticles (Shahjahan *et al.,* 2017).

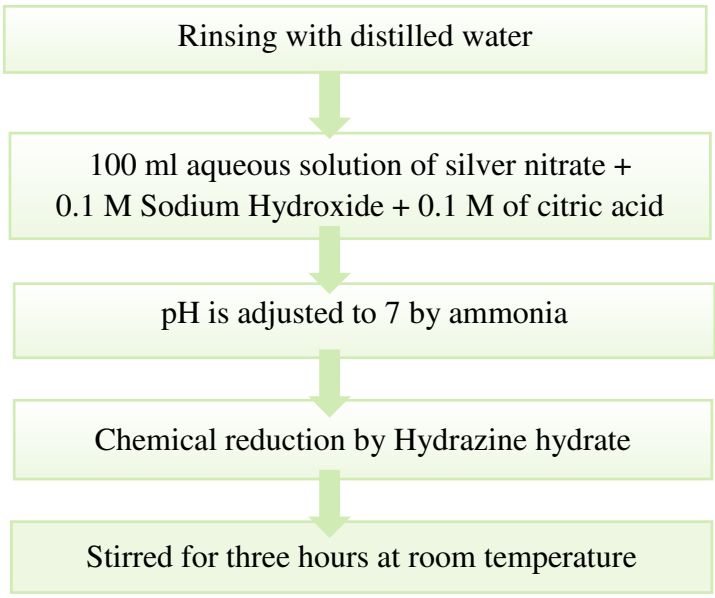

Fig. 1: Flow diagram of Ag nanoparticle synthesis.

Fig. 2: Prepared Nano particles of 1st sample.

The prepared nanoparticles are shown in **Fig. 2**. The weight fraction of the nanofluid was 0.72%; that is, 1.8 gm of nanoparticles was used to make 250 ml of nanofluid.

Chemical Compositions

A total of three samples were made where the silver nanoparticle or $AgNO_3$ concentration was increased, as was the concentration of the reducing agent gradually, as shown in **Table 1**. Silver nitrate, silver chloride, silver carbonate and silver sulfate can also be used with different approaches for the reduction of ions. However, in wet chemistry for reducing silver, silver nitrate and silver perchlorate are usually used, which, when reduced using a reduction agent, can form colloids.

Table 1: Summary of the chemical compositions of the prepared samples.

	$AgNO_3$	$C_6H_8O_7$	NaOH	$N_2H_4.H_20$
1st Sample	50 mM	0.8 M	1 M	200 mM
2nd Sample	60 mM	1 M	1 M	300 mM
3rd Sample	80 mM	1.25 M	1 M	500 mM

Sodium hydroxide accelerates this process and the particle size of silver nanoparticles also changes depending upon the concentration of sodium hydroxide (Shahjahan *et al.,* 2017). Citric acid works as a complexing agent, stabilizer and reducing agent. Researchers believe that it also helps in the shape and size formation of silver nanoparticles (Jiang *et al.,* 2010). Hydrazine hydrate, which plays the role of a reducer, reduces silver to silver ions. After creating a mixture of silver nitrate, sodium hydroxide and citric acid, the solution became acidic as the pH of the solution remained 3-5, and the pH was adjusted to 7 by the addition of ammonia.

Ultrasonication and dispersion

The ultrasonication process uses sound energy at very high frequencies to break apart particle agglomerates by implosion and expansion of bubbles and by cavitation. Ultrasonication is used to disperse the nanofluids in base fluids by using ultrasonic waves and after mixing with water, the particles are kept in an ultrasonic cleaner.

Confirmation of silver particles

The presence of silver crystallite particles was confirmed by comparison with an ideal XRD pattern of silver nanoparticles. Usually, for research

purposes, the curve is compared with the International Center of Diffraction Data (ICDD) database and/or with the data of other researchers. The XRD pattern of sample 1 shown in **Fig. 3** and compared with the XDR graph found in the research paper are shown in **Fig. 4** (Singh *et al.,* 2014). Along with the silver nanoparticle powder, there were traces of sodium hydroxide, citric acid, ammonia and hydrazine hydrate in the primary solution.

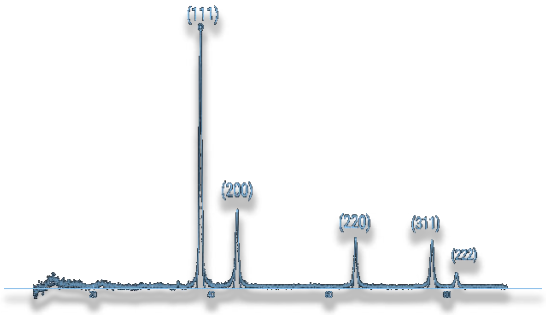

Fig. 3: The XRD graph of the sample 1.

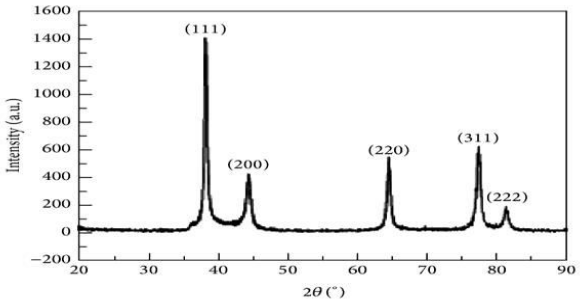

Fig. 4: The XRD graph for Ag nano particle from research paper.

The standard XRD pattern shows peaks at 2Θ angles of $^{38°}$, $^{44°}$, $^{64°}$, $^{77°}$, and 82°, which approximately match the XRD pattern of our samples. The silver crystal structure yields peaks for five planes with plane numbers of (111), (200), (220), (311) and (222).

XRD test

The XRD peak information was extracted to calculate the crystallite size using the following Scherrer equation:

$$D = \frac{k\lambda}{\beta \cos\theta}$$

Where D = the crystallite size in nanometers and k = the dimensionless shape factor. The typical values are approximately 0.9, $\lambda =$ 0.15406 (for Cu K alpha), $\beta =$ Full width at half maximum, and $\cos\theta$ = Peak Position = Two theta angle. This angle is also called the Bragg angle, which provides coherent and incoherent scattering, and the Bragg equation is written as follows:

$$2\,d\,sin\,\theta = n\lambda$$

Where n = positive integer and d = interplanar distance.

Heat Transfer

The heat transfer coefficient test was performed using a shell and tube heat exchanger where the material of the tube was copper, which was coiled inside the shell, and the material of the shell was acrylic. The flow of the nanofluids in the heat exchanger was natural because of the gravitational force, as it was a vertical shell and tube. The heat transfer coefficient was measured using the logarithmic mean temperature difference (LMTD) method. The following equation governs the measurement of the heat transfer coefficient via the LMTD method.

$$\dot{Q} = h.A.\Delta T_{\mathrm{m}}$$

Where h = heat transfer coefficient, A = area of the transfer region, and ΔT_{LMTD} = logarithmic temperature difference.

$$\Delta T_{\mathrm{m}} = \frac{\Delta T_A - \Delta T_B}{\ln\left(\frac{T_A}{T_B}\right)}$$

$$\Delta T_A = T_{hot,in} - T_{cold,out}$$

$$\Delta T_B = T_{hot,out} - T_{cold,in}$$

$T_{cold,in}$ is the room temperature, which was measured with a thermocouple; the data after every second were logged into a computer using a data logger, and the average of all the data were taken for calculation. $T_{hot,in}$ was also measured with a thermocouple, and the data were taken in the same way as $T_{cold,out.}$. $T_{hot,out}$ was not measurable because it was a shell and tube heat exchanger, and inserting a thermocouple at the bottom of the bottle would have been risky because it could result in fluid loss. Therefore, the energy balance equation was used to determine $T_{hot,out}$ temperature as follows:

$$Q = \dot{m}\dot{S}\Delta\theta$$

The ΔT hot, out temperature was determined by equilibrating the hot fluid and the cold fluid.

ΔTLMTD was corrected using the correction factor following the procedure described below:

$$p = \frac{T_{cold,out} - T_{cold,in}}{T_{hot,out} - T_{cold,in}}$$

$$R = \frac{T_{hot,in} - T_{hot,out}}{T_{cold,out} - T_{cold,in}}$$

$$X = \frac{1 - (\frac{RP-1}{P-1})^{\frac{1}{N}}}{R - (\frac{RP-1}{P-1})^{\frac{1}{N}}}$$

$$F = \frac{(\frac{\sqrt{(R^2+1)}}{R^2-1}) \ln(\frac{1-X}{1-RX})}{\ln\frac{\frac{2}{X} - 1 - R + \sqrt{(R^2+1)}}{\frac{2}{X} - 1 - R - \sqrt{(R^2+1)}}}$$

Here, P = the temperature change in the cold fluid divided by the maximum temperature difference, R= the temperature change ratio of the hot and cold streams, X= the nondimensional number, N=the number of shells, F= the correction factor,

Corrected LMTD = F × ΔTm (JOLLIFFE *et al.*, 1940)

RESULTS AND DISCUSSION:

XRD results and analysis

The following graphs show the XRD results for the different samples, and the curves were analyzed using the software "fityk". There was no noticeable difference in the pattern determined from the fitted curve, as shown in **Fig. 5**, compared with the unfitted curve shown in **Fig. 6**. The Ag nanoparticle size for all the samples was calculated similarly to the calculation shown in **Table 1** for sample 1.

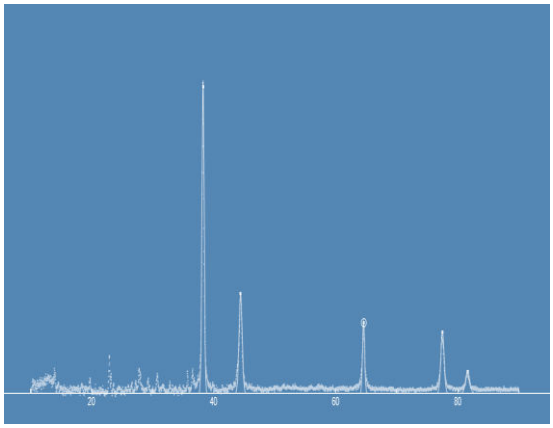

Fig. 5: The unfitted graph for the 1st sample.

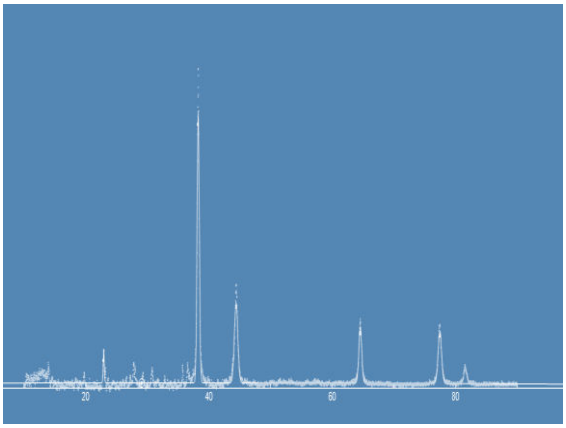

Fig. 6: The fitted graph for the 1st sample.

Table 2: Crystallite size calculation from the fitted and unfitted curves of the 1st sample.

Unfitted Curve (1st Sample)								
Peak Count.	K	λ	FWHM (deg)	β	2 Θ	Θ (rad)	CosΘ	D nm
1st	0.9	0.15406	0.483086	0.008431	38.1716	0.33311	0.94503	17.40143
2nd	0.9	0.15406	0.52	0.009076	44.35	0.387027	0.926035	16.49773
3rd	0.9	0.15406	0.52	0.009076	64.5	0.562869	0.845728	18.0643
4th	0.9	0.15406	0.6	0.010472	77.41	0.67553	0.780376	16.9668
5th	0.9	0.15406	0.6	0.010472	81.54	0.711571	0.757337	17.48294
							Avg D	17.28264
Fitted Curve (1st Sample)								
Peak Count.	K	λ	FWHM (deg)	β	2 Θ	Θ (rad)	CosΘ	D nm
1st	0.9	0.15406	0.483086	0.008431	38.1716	0.33311	0.94503	17.40143
2nd	0.9	0.15406	0.786537	0.013728	44.327	0.386826	0.926111	10.90618
3rd	0.9	0.15406	0.72594	0.01267	64.4941	0.562817	0.845755	12.93926
4th	0.9	0.15406	0.830894	0.014502	77.4042	0.675479	0.780407	12.25146
5th	0.9	0.15406	1.04918	0.018312	81.5261	0.711449	0.757416	9.997016
							Avg D	12.69907
						Total	Average D	15

With increasing concentration, the size of the nanoparticles increased, which was consistent with previous results. The crystallite sizes of the 1st, 2nd and 3rd samples were averaged from the fitted and unfitted data and were found to be 15.07 nm, 19.90 nm and 21.25 nm, respectively. However, increasing the concentration by 10 times did not significantly change the particle size.

Heat Transfer Coefficient

The temperature of the fluid entering the heat exchanger was 18°C for the base fluid as well as for the nanofluids, and the temperature of the hot fluid ranged from 80°C to 85°C. The heat transfer coefficient calculation was shown for the base fluid in **Table 3**; similarly, the remainder of the heat transfer coefficient was calculated.

Table 3: Heat transfer coefficient of the base fluid.

T (hot, in)	85 °C	ΔTm	48.42 °C
T (hot, out)	70 °C	C. LMTD	47.36
T (cold, in)	18 °C	D (m)	0.07
T (cold, out)	40 °C	L (m)	1.55
Q (W)	43869	A (m^2)	0.32
		h (W/m^2K)	2926.84

The heat transfer coefficient of the base fluid (water) is 2926.85 $W/(m^2K)$, and the heat transfer coefficients with nanoparticles for samples 1, 2 and 3 are 4928.22 $W/(m^2K)$, 5125.26 $W/(m^2K)$ and 4629.25 $W/(m^2K)$, respectively.

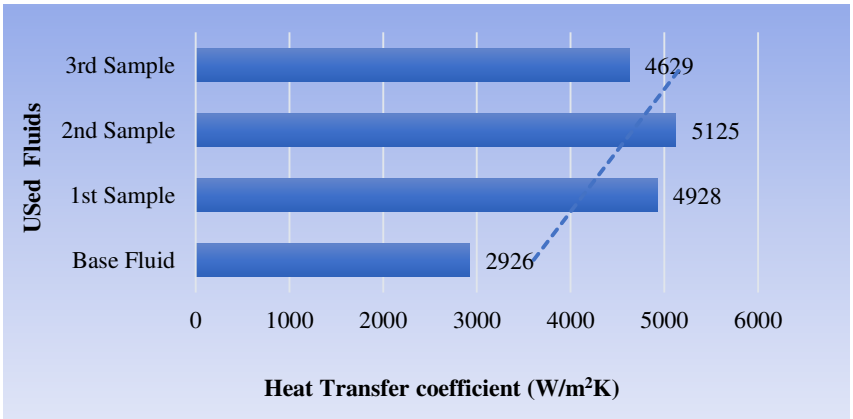

Fig. 7: Comparative chart for heat transfer coefficients.

As almost all the previous research shows, by adding nanoparticles to the base fluid, the heat transfer coefficient of nanofluids increases, as expected. The overall comparison of heat transfer vs fluid is shown in **Fig. 7**. The results for the 1st and 2nd samples are promising, whereas that for the 3rd sample is slightly lower. This could be due to improper dispersion during nanofluid mixing, and further research could clarify this phenomenon.

CONCLUSION:

Three samples of silver nanoparticles 15 nm, 20 nm and 21 nm in size were synthesized for this study, and it was found that the silver nanoparticle size increased with increasing concentration and addition of silver nitride. Adding nanoparticles to a base fluid also increases the heat transfer coefficient of that base fluid. The increases in the heat transfer coefficient for the 1st, 2nd and 3rd samples are 68%, 75% and 58%, respectively, greater than that of the base fluid. However, the extent of heat transfer is not satisfactory because there are other metal nanoparticles, such as copper nanoparticles, which also have similar heat transfer coefficients (Luna *et al.*, 2015).

AUTHOR CONTRIBUTIONS:

M.A.S. Data collection, Analysis and interpretation of results, and Manuscript preparation; M.A.I. Data collection, Manuscript writing and review; S.S. Data collection, Manuscript writing and review; M.A.S. Study conception and design, Manuscript review; M.A.I. and S.S. Study conception and design, Analysis and interpretation of results, Manuscript writing and review.

ACKNOWLEDGEMENT:

The Authors would like to thank Dr. M. A. Gaffur, Principle Scientific Officer, Pilot Plant & Process Development Center, Bangladesh Council of Scientific and Industrial Research (BCSIR) for helping and conducting XRD for the project work.

CONFLICTS OF INTEREST:

The authors declare they have no financial interests.

REFERENCES:

1) Anoop, K., Cox, J., & Sadr, R. (2013). Thermal evaluation of nanofluids in heat exchangers. *International Communications in Heat and Mass Transfer*, **49**, 5-9. https://doi.org/10.1016/j.icheatmasstransfer.2013.10.002
2) Arya, A., Mishra, V., & Chundawat, T. S. (2019). Green Synthesis of Silver Nanoparticles from Green Algae (Botryococcus braunii) and its Catalytic Behavior for the Synthesis of Benzimidazoles. *Chemical Data Collections*, 100190. https://doi.org/10.1016/j.cdc.2019.100190
3) Bian, H., Zhang, X., & Zhang, N. (2019). Controlled synthesis of silver nanoparticles from polyoxometalates-immobilized poly (4-vinylpyridine) brushes. *Chinese Chemical Letters*. https://doi.org/10.1016/j.cclet.2019.01.030
4) Bokov, Dmitry, Turki Jalil, & Kianfar, Ehsan (2021). Nanomaterial by Sol-Gel Method: Synthesis and Application, *Advances in Materials Science and Engineering*, 2021, 5102014, 21 pages, 2021. https://doi.org/10.1155/2021/5102014
5) Chibac, A., Melinte, V., & Buruiana, E. C. (2012). One-pot synthesis of photo cross linked sol-gel hybrid composites containing silver nanoparticles in urethane-acrylic matrixes. *Chemical Engineering Journal*, 200-202, 577-588. https://doi.org/10.1016/j.cej.2012.06.110
6) Choi, S. U. S. (2008). Nanofluids: A new field of scientific research and innovative applications. *Heat Transfer Engineering*, **29**(5), 429-431. https://doi.org/10.1080/01457630701850778
7) Cui, Y., Wang, J., & Yin, N. (2018). Formation of silver nanoparticles by human gut microbiota. *Science of the Total Environment*, **651**, 1489-1494. https://doi.org/10.1016/j.scitotenv.2018.09.312
8) Das, S., Giri, Dr. A., & Kanagaraj, Dr. S. (2019). Role of graphene nanofluids on heat transfer enhancement in thermosyphon. *Journal of Science: Advanced Materials and Devices*. https://doi.org/10.1016/j.jsamd.2019.01.005
9) Das, S. K., Choi, S. U. S., & Patel, H. E. (2006). Heat transfer in nanofluids - A review. *Heat Transfer Engineering*, **27**(10), 3-19. https://doi.org/10.1080/01457630600904593
10) Edworthy, I. S., Rodden, M., & Arnold, P. L. (2005). Silver alkoxide and amino N-heterocyclic carbenes; Syntheses and crystal structures. *Journal of Organometallic Chemistry*, **690**(24-25), 5710-5719. https://doi.org/10.1016/j.jorganchem.2005.07.063
11) Escobar-Hernández, J. M. A., & Escobar-Remolina, J. C. M. (2019). Silver nanoparticles: Synthesis and mathematical-geometric formulation. *Nano-Structures and Nano-Objects*, **17**, 259-268. https://doi.org/10.1016/j.nanoso.2019.01.005
12) Hosseini, K., & Ghorbani, H. R. (2018). Silver/oil nanofluids in heat exchanger an experimental study on convective heat transfer. *Oriental Journal of Chemistry*, **34**(2), 1126–1129. https://doi.org/10.13005/ojc/340266
13) Huminic, G., & Huminic, A. (2018). Heat transfer capability of the hybrid nanofluids for heat transfer applications. *Journal of Molecular Liquids*, **272**, 857-870. https://doi.org/10.1016/j.molliq.2018.10.095
14) Islam T., Akter N., and Jahan N. (2020). MHD free convective heat transfer in a triangular enclosure filled with Copper-water nanofluid, *Int. J. Mat. Math. Sci*., **2**(2), 29-38. https://doi.org/10.34104/ijmms.020.029038
15) Jiang, X. C., Chen, C. Y., & Yu, A. B. (2010). Role of citric acid in the formation of silver nanoplates through a synergistic reduction approach. *Langmuir*, **26**(6), 4400-4408. https://doi.org/10.1021/la903470f
16) Jolliffe, N., Bowman, K. M., & Fein, H. D. (1940). Nicotinic acid deficiency encephalopathy. *JAMA*, **114**(4), 307-312. https://doi.org/10.1001/jama.1940.02810040017004
17) King, S., Jarvie, H., & Dobson, P. (2024). nanoparticle. Encyclopædia Britannica, Inc. https://www.britannica.com/science/nanoparticle
18) Luna, I. Z., Chowdhury, A. M. S., & Khan, R. A. (2015). Measurement of Forced Convective Heat Transfer Coefficient of Low Volume Fraction

CuO-PVA Nanofluids under Laminar Flow Condition. **3**(2), 64-67. https://doi.org/10.12691/ajn-3-2-3

19) Mahdieh, M., Zolanvari, A., & Mahdieh, M. (2012). Green biosynthesis of silver nano-particles by Spirulina platensis. *Scientia Iranica*, **19**(3), 926-929. https://doi.org/10.1016/j.scient.2012.01.010

20) Michna, A., Morga, M., & Kubiak, K. (2019). Monolayers of silver nanoparticles obtained by green synthesis on macrocation modified substrates. *Materials Chemistry and Physics*. https://doi.org/10.1016/j.matchemphys.2019.01.072

21) Noroozi, M., Radiman, S., & Soltaninejad, S. (2014). Fabrication, characterization, and thermal property evaluation of silver nanofluids. *Nanoscale Research Letters*, **9**(1), 1-10. https://doi.org/10.1186/1556-276X-9-645

22) Pontaza-Licona, Y. S., Ramos-Jacques, A. L., & Hernandez-Martínez, A. R. (2019). Alcoholic extracts from Paulownia tomentosa leaves for silver nanoparticles synthesis. *Results in Physics*, **12**, 1670-1679. https://doi.org/10.1016/j.rinp.2019.01.082

23) Raj, S., Chand Mali, S., & Trivedi, R. (2018). Green synthesis and characterization of silver nanoparticles using Enicostemma axillare (Lam.) leaf extract. *Biochemical and Biophysical Research Communications*, **503**(4), 2814-2819. https://doi.org/10.1016/j.bbrc.2018.08.045

24) Rodrigues, N. L., Fontes, D. H., & Bandarra Filho, E. P. (2014). A review on applications of nanofluids in automotive cooling system. Encit 2014, 445001(*15th Brazilian Congress of Thermal Sciences and Engineering*), 7. https://doi.org/10.13140/RG.2.1.3109.5207

25) Roszko, A., Fornalik-Wajs, E., & Kenjeres, S. (n.d.). Magneto-thermal convection of low concentration nanofluids. https://doi.org/10.1051/matecconf/20141803006

26) Shahjahan, M., Rahman, M. H., & Begum, M. H. A. (2017). Synthesis and Characterization of Silver Nanoparticles by Sol-gel Technique. *Nanoscience and Nanometrology*, **3**(10), 5455-5461. https://doi.org/10.11648/j.nsnm.20170301.16

27) Singh, R., Sahu, S. K., & Thangaraj, M. (2014). Biosynthesis of Silver Nanoparticles by Marine Invertebrate (Polychaete) and Assessment of Its Efficacy against Human Pathogens. *Journal of Nanoparticles*. 1-7. https://doi.org/10.1155/2014/718240

28) Solanki, J. N., & Murthy, Z. V. P. (2011). Preparation of silver Nanofluids with High Electrical Conductivity. *J. of Dispersion Science and Technology*, **32**(5), 724-730. https://doi.org/10.1080/01932691.2010.480863

29) Wanarska, E., & Maliszewska, I. (2019). The possible mechanism of the formation of silver nanoparticles by Penicillium cyclopium. Bio-organic Chemistry, February, 1-9. https://doi.org/10.1016/j.bioorg.2019.02.028

30) Wang, L., & Wei, X. (2009). Nanofluids: Synthesis, Heat Conduction, and Extension. *J. of Heat Transfer*, **131**(3), 033102. https://doi.org/10.1115/1.3056597

31) Zheng, K., & Boccaccini, A. R. (2017). Sol-gel processing of bioactive glass nanoparticles: A review. Advances in Colloid and Interface Science, **249**, 363-373. https://doi.org/10.1016/j.cis.2017.03.0008

Citation: Shahriar MA, Islam MA, and Saha S. (2024). Heat transfer analysis using synthesized silver nanoparticles, *Int. J. Mat. Math. Sci.*, **6**(4), 112-119. https://doi.org/10.34104/ijmms.024.01120119